Available online at www.sciencedirect.com
ScienceDirect
Astroparticle Physics 26 (2006) 129–139
Astroparticle Physics
www.elsevier.com/locate/astropart

Limits on the muon flux from neutralino annihilations at the center of the Earth with AMANDA

A. Achterberg [y], M. Ackermann [aa], J. Adams [h], J. Ahrens [p], K. Andeen [o], D.W. Atlee [w], J.N. Bahcall [s,✠], X. Bai [r], B. Baret [f], M. Bartelt [j], S.W. Barwick [k], R. Bay [c], K. Beattie [d], T. Becka [p], J.K. Becker [j], K.-H. Becker [z], P. Berghaus [e], D. Berley [i], E. Bernardini [aa], D. Bertrand [e], D.Z. Besson [l], E. Blaufuss [i], D.J. Boersma [o], C. Bohm [u], S. Böser [aa], O. Botner [x], A. Bouchta [x], O. Bouhali [e], J. Braun [o], C. Burgess [u], T. Burgess [u], T. Castermans [q], D. Chirkin [d], J. Clem [r], J. Conrad [x], J. Cooley [o], D.F. Cowen [w,v], M.V. D'Agostino [c], A. Davour [x], C.T. Day [d], C. De Clercq [f], P. Desiati [o], T. DeYoung [w], J.C. Diaz-Velez [o], J. Dreyer [j], M.R. Duvoort [y], W.R. Edwards [d], R. Ehrlich [i], P. Ekström [u], R.W. Ellsworth [i], P.A. Evenson [r], O. Fadiran [a], A.R. Fazely [b], T. Feser [p], K. Filimonov [c], T.K. Gaisser [r], J. Gallagher [n], R. Ganugapati [o], H. Geenen [z], L. Gerhardt [k], A. Goldschmidt [d], J.A. Goodman [i], R. Gozzini [p], M.G. Greene [w], S. Grullon [o], A. Groß [j], R.M. Gunasingha [b], M. Gurtner [z], A. Hallgren [x], F. Halzen [o], K. Han [h], K. Hanson [o], D. Hardtke [c], R. Hardtke [t], T. Harenberg [z], J.E. Hart [w], T. Hauschildt [r], D. Hays [d], J. Heise [y], K. Helbing [z], M. Hellwig [p], P. Herquet [q], G.C. Hill [o], J. Hodges [o], K.D. Hoffman [i], K. Hoshina [o], D. Hubert [f], B. Hughey [o], P.O. Hulth [u], K. Hultqvist [u], S. Hundertmark [u], J.-P. Hülß [z], A. Ishihara [o], J. Jacobsen [d], G.S. Japaridze [a], A. Jones [d], J.M. Joseph [d], K.-H. Kampert [z], A. Karle [o], H. Kawai [g], J.L. Kelley [o], M. Kestel [w], S.R. Klein [d], S. Klepser [aa], G. Kohnen [q], H. Kolanoski [aa,1], L. Köpke [p], M. Krasberg [o], K. Kuehn [k], H. Landsman [o], H. Leich [aa], M. Leuthold [aa], I. Liubarsky [m], J. Lundberg [x], J. Madsen [t], P. Marciniewski [x], K. Mase [g], H.S. Matis [d], T. McCauley [d], C.P. McParland [d], A. Meli [j], T. Messarius [j], P. Mészáros [w,v], Y. Minaeva [u], P. Miočinović [c], H. Miyamoto [g], A. Mokhtarani [d], T. Montaruli [o,2], A. Morey [c], R. Morse [o], S.M. Movit [v], K. Münich [j], R. Nahnhauer [aa], J.W. Nam [k], T. Neunhöffer [p], P. Nießen [r], D.R. Nygren [d], H. Ögelman [o], Ph. Olbrechts [f], A. Olivas [i], S. Patton [d], C. Peña-Garay [s], C. Pérez de los Heros [x], A. Piegsa [p], D. Pieloth [aa], A.C. Pohl [x,3], R. Porrata [c], J. Pretz [i], P.B. Price [c], G.T. Przybylski [d], K. Rawlins [o], S. Razzaque [v], F. Refflinghaus [j], E. Resconi [aa], W. Rhode [j], M. Ribordy [q], A. Rizzo [f], S. Robbins [z], J. Rodríguez Martino [u], C. Rott [w], D. Rutledge [w], H.-G. Sander [p], S. Schlenstedt [aa], D. Schneider [o], R. Schwarz [o], D. Seckel [r], S.H. Seo [w], S. Seunarine [h], A. Silvestri [k], A.J. Smith [i], M. Solarz [c], C. Song [o], J.E. Sopher [d], G.M. Spiczak [t],

[*] Corresponding author. Tel.: +46 8 5537 8664; fax: +46 8 5537 8601.
E-mail address: walck@physto.se (C. Walck).
[✠] Deceased.
[1] Affiliated with Insitut für Physik, Humboldt Universität zu Berlin, D-12489 Berlin, Germany.
[2] Affiliated with Università di Bari, Dipartimento di Fisica, I-70126, Bari, Italy.
[3] Affiliated with Department of Chemistry and Biomedical Sciences, Kalmar University, S-39182 Kalmar, Sweden.

0927-6505/$ - see front matter
doi:10.1016/j.astropartphys.2006.05.007

C. Spiering [aa], M. Stamatikos [o], T. Stanev [r], P. Steffen [aa], T. Stezelberger [d], R.G. Stokstad [d], M.C. Stoufer [d], S. Stoyanov [r], E.A. Strahler [o], K.-H. Sulanke [aa], G.W. Sullivan [i], T.J. Sumner [m], I. Taboada [c], O. Tarasova [aa], A. Tepe [z], L. Thollander [u], S. Tilav [r], P.A. Toale [w], D. Turčan [i], N. van Eijndhoven [y], J. Vandenbroucke [c], B. Voigt [aa], W. Wagner [j], C. Walck [u,*], H. Waldmann [aa], M. Walter [aa], Y.-R. Wang [o], C. Wendt [o], C.H. Wiebusch [z], G. Wikström [u], D.R. Williams [w], R. Wischnewski [aa], H. Wissing [aa], K. Woschnagg [c], X.W. Xu [o], G. Yodh [k], S. Yoshida [g], J.D. Zornoza [o,4]

[a] *CTSPS, Clark-Atlanta University, Atlanta, GA 30314, USA*
[b] *Depatment of Physics, Southern University, Baton Rouge, LA 70813, USA*
[c] *Department of Physics, University of California, Berkeley, CA 94720, USA*
[d] *Lawrence Berkeley National Laboratory, Berkeley, CA 94720, USA*
[e] *Université Libre de Bruxelles, Science Faculty CP230, B-1050 Brussels, Belgium*
[f] *Vrije Universiteit Brussel, Dienst ELEM, B-1050 Brussels, Belgium*
[g] *Department of Physics, Chiba University, Chiba 263-8522, Japan*
[h] *Department of Physics and Astronomy, University of Canterbury, Private Bag 4800, Christchurch, New Zealand*
[i] *Department of Physics, University of Maryland, College Park, MD 20742, USA*
[j] *Department of Physics, Universität Dortmund, D-44221 Dortmund, Germany*
[k] *Department of Physics and Astronomy, University of California, Irvine, CA 92697, USA*
[l] *Department of Physics and Astronomy, University of Kansas, Lawrence, KS 66045, USA*
[m] *Blackett Laboratory, Imperial College, London SW7 2BW, UK*
[n] *Department of Astronomy, University of Wisconsin, Madison, WI 53706, USA*
[o] *Department of Physics, University of Wisconsin, Madison, WI 53706, USA*
[p] *Institute of Physics, University of Mainz, Staudinger Weg 7, D-55099 Mainz, Germany*
[q] *University of Mons-Hainaut, 7000 Mons, Belgium*
[r] *Bartol Research Institute, University of Delaware, Newark, DE 19716, USA*
[s] *Institute for Advanced Study, Princeton, NJ 08540, USA*
[t] *Department of Physics, University of Wisconsin, River Falls, WI 54022, USA*
[u] *Department of Physics, Stockholm University, SE-10691 Stockholm, Sweden*
[v] *Department of Astronomy and Astrophysics, Pennsylvania State University, University Park, PA 16802, USA*
[w] *Department of Physics, Pennsylvania State University, University Park, PA 16802, USA*
[x] *Division of High Energy Physics, Uppsala University, S-75121 Uppsala, Sweden*
[y] *Department of Physics and Astronomy, Utrecht University/SRON, NL-3584 CC Utrecht, The Netherlands*
[z] *Department of Physics, University of Wuppertal, D-42119 Wuppertal, Germany*
[aa] *DESY, D-15735, Zeuthen, Germany*

Received 24 January 2006; received in revised form 27 April 2006; accepted 24 May 2006
Available online 5 July 2006

Abstract

A search has been performed for nearly vertically upgoing neutrino-induced muons with the Antarctic Muon And Neutrino Detector Array (AMANDA), using data taken over the three year period 1997–99. No excess above the expected atmospheric neutrino background has been found. Upper limits at 90% confidence level have been set on the annihilation rate of neutralinos at the center of the Earth, as well as on the muon flux at AMANDA induced by neutrinos created by the annihilation products.

Keywords: Dark matter; Neutrino telescopes; AMANDA; IceCube; Neutralino

1. Introduction

One of the most challenging problems in cosmology today is that of dark matter, the presence of which has been inferred from observations of the mass distributions of galaxies and clusters of galaxies. This led to the concordance model, which stipulates that 23% of the Universe is made up of non-baryonic cold dark matter (CDM). This model has been supported by observations of the cosmic microwave background radiation [1].

There are a number of theoretical candidates for the CDM, the favored one is a weakly interacting massive par-

[4] Affiliated with IFIC (CSIC-Universitat de València), AC 22085, 46071 Valencia, Spain.

ticle (WIMP). WIMPs are postulated to be non-relativistic relic particles with masses in the range from tens of GeV to a few TeV, which decoupled from the thermal equilibrium in the early universe. Among several plausible WIMP scenarios, the lightest supersymmetric particle (LSP) in supersymmetric extensions to the standard model of particle physics is the most widely studied. Such a particle would be stable if R-parity is conserved. If the LSP is a Majorana particle, as in the case of the neutralino, then such particles could annihilate pairwise. Such WIMPs could be detected either directly through elastic scattering on nuclei in an instrumented target volume, or indirectly, by detecting the products of the annihilation process or secondaries from their decays.

The present paper concerns a search for neutrino-induced muons from neutralino annihilations at the center of the Earth. The data are compared to the minimal supersymmetric extension of the standard model (MSSM) detailed in [2], which provides the neutralino as the WIMP dark matter candidate. Within the MSSM, the neutralino is the lightest, stable particle. It is a linear combination of the neutral gauginos $\widetilde{B}$, $\widetilde{W}_3$ and the neutral Higgsinos $\widetilde{H}_1^0$, $\widetilde{H}_2^0$. Neutralinos can scatter off nuclei in the Earth, and if enough energy is lost in the interaction they will become gravitationally trapped. The captured neutralinos will accumulate at the center of the Earth after additional scatterings, where they can annihilate and generate neutrinos. These neutrinos can subsequently produce muons through charged current interactions. The dominant background to this neutrino signal from the center of the Earth is caused by cosmic rays interacting in the atmosphere above the detector, with atmospheric muons being created in the resulting air showers. A secondary, but almost irreducible, background is muons induced by atmospheric neutrinos originating in cosmic ray showers on the opposite side of the Earth. The neutralino signal needs to be distinguished from these two backgrounds.

Buried deep in the Antarctic glacial ice beneath the Amundsen–Scott South Pole Station, the Antarctic Muon And Neutrino Detector Array (AMANDA) consists of 677 optical modules (OMs). The OMs are made of 8 in. photomultiplier tubes (PMTs) encased in glass spheres that act as pressure vessels. The OMs that are mounted on the lowest five to seven hundred meters of two-and-a-half-kilometer long cables. These are used for supplying the high voltage to the PMTs as well as for retrieving the PMT signals. During the data taking period discussed in this paper 10–13 strings were instrumented. In 2000 the detector was complete, with a total of 19 strings, arranged on two concentric circles with diameters of 120 and 200 m. More details on the detector can be found in Ref. [3]. The multiplicity trigger condition in 1997 required hits in at least 16 OMs within a time window of 2 μs, in 1998 the requirement was at least 12 OMs and in 1999 at least 18 OMs.

A dark matter search has been performed with AMANDA using data collected during 1997–1999. This improved analysis [4] yields results which supersede the earlier limits given by AMANDA in Ref. [5]. The signal and background simulations performed for the new analysis are discussed in Section 2. In Section 3, the data sets as well as the improved analysis methods are presented. As a cross check, an independent analysis of data taken in 1999 [6] is presented in Section 4; the results are compared to those of the full three year analysis. The steps involved in the calculation of the muon flux limits are summarized in Section 5, and the final results and a comparison to other experiments are discussed in Sections 5 and 6. The AMANDA collaboration has also recently published a dark matter search for neutralino annihilation in the centre of the Sun [7].

2. Simulation of signal and backgrounds

The event simulation is performed in three separate steps. Muon samples are created with various generation programs, and are subsequently propagated to the vicinity of the detector with muon propagation software. The detector response to the light emitted by the muons is then simulated to produce events that trigger the AMANDA detector.

2.1. Neutralino annihilations at the center of the Earth

The high energy muon neutrinos created in neutralino annihilations at the center of the Earth are generated with the WIMPSIMP code [8]. Signal event samples were created for seven hypothetical neutralino masses ranging from 50 to 5000 GeV/c^2, and for two different annihilation channels at each mass: the W^+W^- channel (in the case 50 GeV/c^2 the $\tau^+\tau^-$ channel) is used for the hard annihilation spectrum and the $b\bar{b}$ channel for the soft spectrum. This choice follows earlier work [5,9] and represents two extreme cases of the neutrino energy spectrum.

In the calculation of the neutralino capture rates, the local dark matter energy density is assumed to be 0.3 GeV/cm^3. The input to the WIMPSIMP code are tables with 1.25×10^6 events produced through Monte Carlo simulations of the annihilation process with an approximate treatment of the hadronization [9].

PYTHIA [10] (version 6.215) is used for the detailed simulation of the neutrino-nucleon interaction. The average momentum direction and the total energy of all the other particles created in the hadronic shower, besides the muon, were calculated for use in the detector simulation. The hadronic shower is particularly important for the detection of events with low energy muons, as the extra light from the shower allows events to pass the trigger multiplicity threshold where the light from the muon alone would not have sufficed. These low energy muons are central in the analysis of low neutralino mass scenarios.

2.2. Atmospheric neutrinos

The atmospheric neutrino generation is performed with the NUSIM Monte Carlo code [11]. Neutrinos and

anti-neutrinos are treated separately using the corresponding cross sections. The neutrino-nucleon interaction cross sections are calculated using the MRS-G parton distributions [12].

Muons with energies in the range from 10 to 10^8 GeV and with zenith angles between 80° and 180° are considered in the background simulation. A total of 1.2×10^8 atmospheric neutrino events have been simulated for this work, divided equally over the three years due to the slightly different detector configurations.

2.3. Atmospheric muons

The air showers – in which the atmospheric muons are generated – are simulated with CORSIKA [13,14] (version 6.020). The input is a cosmic ray spectrum with spectral index $\gamma = 2.7$ and the measured particle composition as described in [15]. For the high energy hadronic interactions, the QGSJET model [16] has been used. The primaries are simulated with energies between 600 and 10^{11} GeV, with a low energy cutoff for the primaries which is proportional to the atomic weight of the primary particle. In the simulation, the Earth's curvature is taken into account along with the atmospheric profile and magnetic field at the South Pole. The muons are generated on a surface just below the ground level, at a depth of 35 m, in order to compensate for the low-density firn layer on top of the ice. Every muon event is oversampled 10 times through random redistribution at this surface level. In this work a total of 1.42×10^{13} showers was generated, corresponding to a livetime of 649.6 days. Roughly following the livetime distribution of the collected data, this sample is divided over the three years such that 128.5 days were simulated for the 1997 detector configuration, 246.8 days for 1998 and 274.2 days for 1999.

2.4. Muon propagation and detector response

The propagation of the generated muons is performed by the MMC (Muon Monte Carlo) program [17], which accounts for ionization of the ice, bremsstrahlung, production of δ-electrons, muon–nucleus interactions, and e^+e^- or $\mu^+\mu^-$ pair production. The energy loss due to the Cherenkov light is negligible. MMC calculations of the energy losses of muons with energies upto 10^{11} GeV are valid to within 1%.

The light deposited by muon energy loss processes is propagated through the ice to the optical modules by the PTD photon simulation [18]. Instead of tracking individual photons, the detector simulation uses lookup tables storing the mean number of photo-electrons and their arrival time distribution, as a function of OM location relative to the light source. These tables take into account the Cherenkov light distribution as well as the specific features of the OMs, e.g. glass and optical gel transparency. The depth dependence of the ice properties – several horizontal dust layers are present in the glacial ice around the detector [19] – is taken into account by using several tables with different ice properties.

The detector response to light emitted by cascades or muons that propagate through or near the array is simulated with the AMASIM program [20]. AMASIM models the PMT response to the light, the cable transport of the PMT signals to the surface and the way these are processed by the data aquisition electronics.

Dark noise has been included in the simulation, with the noise rate of each channel taken from data.

3. Data analysis

The data sample analyzed corresponds to a total livetime of 536.3 days, after removal of runs with abnormal detector behavior. Collected over the three year period 1997–99 it consists of 5.0×10^9 AMANDA triggers. In order to reduce the risk of biasing the analysis a blindness approach has been implemented. Since the search is for neutrino induced muons from the direction of the center of the Earth, which is fixed, the only way to blind the analysis is by sampling the data. The subsample of the data used for establishing the cuts was about 20 percent for each year. A sample of 114.4 days has therefore been used for the selection optimization and is not included in the final results. The remaining sample had a livetime of 421.9 days. Similarly, two sets of simulated events have been produced: the first for use in the selection optimization and the second for the selection efficiency estimations. The analysis consists of six levels of filtering, where each filter level is comprised of cuts on variables derived either directly from the hit pattern in the events or from the event reconstructions [21].

3.1. Filter level 1+2

The recorded events were cleaned of OM signals or 'hits' resulting from noise, unphysically narrow pulses induced by cross talk and OMs that were not operating normally, before the events were reconstructed with maximum likelihood algorithms. As these require a few tenths of a CPU-second per event and as there are of the order of 10^9 events in the data set of each year this means that a full reconstruction of every event would be very time consuming.

To reduce the number of data events to reconstruct, filter level 1 applies a cut on zenith angle approximated by a very fast line fit to the muon track. The line fit uses the time and position of the hit OMs with the assumption that the photons are traversing the detector along a straight line. This fast filtering rejects around 80–90% of the events accepted by the trigger.

The events that pass filter level 1 are then reconstructed with a maximum likelihood algorithm using the line fit as a seed for minimization. At filter level 2 it was required that the reconstructed muon zenith angle be greater than 80° and that the track solution must contain at least three hits with time residuals in the interval from −10 to 25 ns. The

Table 1
The number of events in 421.9 days of data for the simulated atmospheric neutrino (421.9 days equivalent) and atmospheric muon (483.2 days renormalized to 421.9 days) backgrounds as well as the 250 GeV/c^2 hard annihilation channel signal sample that pass the filtering from the trigger level up to filter level 6

Filter level	Data	Atm. neutrinos	Atm. muons	$\chi\bar{\chi} \to W^+W^-$
				$M_\chi = 250$ GeV/c^2
0	3.9×10^9	1.7×10^4	2.7×10^9	1.5×10^5
1+2	3.9×10^7	5.8×10^3	2.5×10^7	8.7×10^4
3	3.1×10^6	3.1×10^3	2.0×10^6	7.4×10^4
4	5.6×10^3	2.9×10^2	7.3×10^3	6.6×10^4
5	1.2×10^2	1.7×10^2	7.9	4.0×10^4
6	9	9.6	0	3.2×10^4

time residual of a hit is defined as the difference between the actual time of the hit and the expected arrival time of an unscattered Cherenkov photon emitted from the reconstructed track. After filter level 1 + 2 the data were reduced by about a factor of one hundred with respect to the triggered events while 51–59% of the signal events remains, see Table 1 for the case of the $M_\chi = 250$ GeV/c^2 hard annihilation channel.

3.2. Filter level 3

At filter level 3 an 'event cleaning' procedure is applied which removes instrumental artifacts that are not included in the simulation. A more elaborate cleaning of hits induced by cross-talk was also implemented in this filter. The events were cleaned of noise hits through exclusion of those hits that were isolated in time or space. Hits from unstable OMs were removed on a run-to-run basis.

At filter level 3 a special technique – direct walk reconstruction – was first used as the initial guess for a Bayesian maximum likelihood algorithm reconstructing a muon trajectory. The zenith dependence corresponding to the atmospheric muon background was used as a prior to weight the likelihood to be maximized. This one-dimensional prior function helps with suppressing the misreconstructions of downgoing muons as upgoing, useful since the flux of downgoing muons is several orders of magnitude larger than that of the upgoing muons. The zenith angle cut at this filter level required that a muon originates below the horizon (90°). A cascade reconstruction was also performed for each event as a secondary hypothesis.

More details on cross-talk cleaning and the reconstruction of AMANDA events can be found in Ref. [21].

3.3. Filter level 4

The aim of filter level 4 is to reduce the downgoing muon background as much as possible while retaining most of the nearly vertically upgoing muons. In order to achieve this a neural network classification scheme is utilized. Individual networks were trained with samples of data (assumed to be pure background) against the signal events for six neutralino masses and two annihilation channels for each of the three years individually making a total of 36 different classifications. The statistics of the signal simulation in the case of the 50 GeV/c^2 channels was too low to allow proper training of the neural networks. Instead, the network and the subsequent cuts developed for the 100 GeV/c^2 hard (soft) annihilation channel were directly applied to the 50 GeV/c^2 hard (soft) channel.

The neural networks used are of the feed-forward multilayer perceptron type [22], typically with 200 adjustable weights, and with eight to ten input nodes. They were chosen from a set of potentially suitable variables through a process of step-wise ranking, and the combinations were systematically tested using a fixed network structure. The zenith angle of the reconstructed muon trajectory – the best discriminator by eye – was chosen as the first input variable. All of the others were tested in combination with the zenith angle in the case of the $M_\chi = 250$ GeV/c^2 hard annihilation channel analysis for 1997 data. The best pair turned out to be the zenith angle and the difference in the number of hits with time residuals in the interval from -15 to 75 ns between the reconstruction with a muon hypothesis and the one with a cascade hypothesis. The other variables were then checked one-by-one together with this pair in the three variable case. The tests continued with combinations of larger number of variables until the improvement in the neural network performance ceased.

The ten input variables chosen for the network optimization procedure are track variables as well as event topological variables, and are listed in Table 2. The number of input variables to use was determined individually for each signal sample by adding or removing one input at the same time as the number of nodes in the hidden layer was optimized by testing every configuration possible. The final

Table 2
The set of variables used as input to the neural networks in filter level 4. See [4] and [21] for more details on the variables and reconstruction methods

- The zenith angle of the reconstructed muon trajectory
- The difference in the number of hits with time residuals in the interval from -15 to 75 ns between the reconstruction with a muon hypothesis and the one with a cascade hypothesis
- The sphericity (shape) of the hits in the event
- The velocity obtained with the line fit
- The greatest distance of one-photo-electron hits from the reconstructed muon trajectory
- The number of strings with hits that have time residuals in the interval from -15 to 75 ns, with respect to the cascade reconstruction
- The smoothness of the distribution of hits that have time residuals in the interval from -15 to 75 ns, with respect to the reconstructed muon trajectory
- The z-coordinate of the 'center of gravity' of the hits
- The absolute difference between the zenith angle of the reconstructed muon trajectory and that of the line fit
- The number of track candidates divided by the number of track hits for the direct walk reconstruction

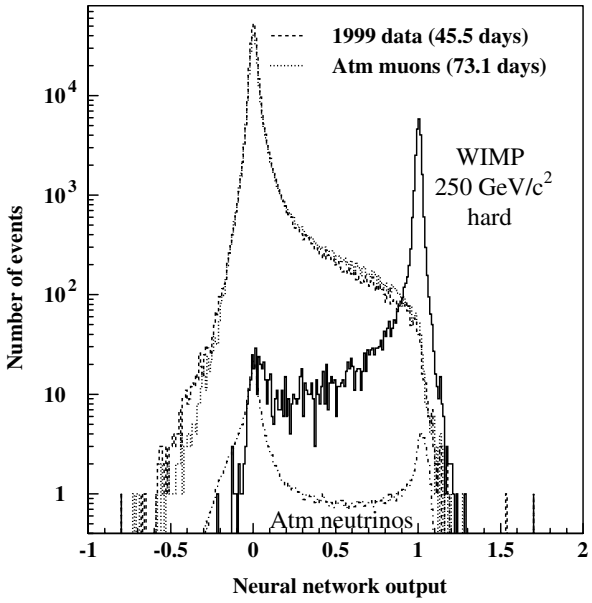

Fig. 1. The output variable of the neural network trained with $M_\chi = 250$ GeV/c^2 hard annihilation channel WIMP signal and 1999 data. All events at filter level 3 for the cut optimization subsets are shown. The WIMP signal is drawn as a solid line, data is dashed, upgoing atmospheric neutrino background is dash-dotted and downgoing muon background is dotted.

number of inputs used in the neural networks ranged from eight to ten.

As an example, the output of the neural network trained with the 250 GeV/c^2 hard annihilation channel WIMP signal and 1999 data is shown in Fig. 1 for the selection optimization samples of the 1999 data, WIMP signal, atmospheric neutrino and atmospheric muon background. A clear separation can be seen for the vast majority of the downgoing atmospheric muons from the WIMP signal events. The fewer atmospheric neutrino events are divided into either signal-like or background-like, illustrating the irreducibility of the atmospheric neutrino background.

3.4. Filter level 5

Although the neural networks are very good at separating signal from background they are limited by the quality of the input variables. In particular, the muon reconstruction at filter level 3 is not perfect and most of the data events that pass the neural network cut are misreconstructed downgoing atmospheric muons that mimic upgoing signal. However, these events have certain characteristics that can be exploited by further filters. The goal of filter level 5 is to remove these 'fakes' so as to obtain a sample which is completely dominated by neutrino-induced upgoing muons.

Some misreconstructions are caused by noise hits that were not cleaned away by the time isolation cut applied in filter level 3 since they consist of pairs or triplets of hits. A new time isolation cut was implemented for level 5 to ignore these hits if they occured more than 500 ns before or after the bulk of hits in the event. A new Bayesian muon reconstruction was performed on the events with this slightly stricter hit cleaning and a zenith cut of 140° applied to the new muon reconstruction.

This is followed by a set of 'quality cuts' designed to remove the other misreconstructed downgoing events in the data. The question of what value of the neural network output to cut on at filter level 4 was addressed through an optimization against the quality cuts in filter level 5. A strong cut on the neural network output value removes the misreconstructed background but also much of the signal sample. Lowering the cut value increases the signal efficiency as well as the background contamination. However, background events of similar nature passed some or all the different neural networks. Different classes of events could be removed by common cuts which increased the signal efficiency as compared to simply applying strong level 4 cuts.

The likelihoods maximized for muons and cascades were ranked lower as neural network variables than the variable "number of hits with time residuals in the interval from −15 to 75 ns", and appeared to be somewhat correlated to it as the combination did not improve the network performance. However, the 'fakes' that pass the level 4 cut often have better cascade than muon likelihoods and are outliers in other distributions as well.

One class of 'fakes' is downgoing muons or muon bundles that either stop just outside the detector or pass by without entering the instrumented volume. Although the resulting light output gives rise to an upward reconstructed muon track, the cascade fit is usually a better solution and the direct walk reconstruction cannot find many track candidates. Another category of misreconstructed events have a good cascade fit, relatively poor muon fit and low line fit velocity.

Most of the well reconstructed events show fair agreement between the solution of the initial fit and the more sophisticated track reconstruction. The space angular difference is therefore a good cut variable. Three variations are used, both between the Bayesian muon likelihood reconstruction and the two different initial fits – the level 1 line fit and the level 3 direct walk fit – as well as between the two initial fits themselves.

The number of late hits – with time residuals greater than 75 ns – can also be correlated with low reconstruction quality. It indicates that the solution did not take into account the topology of the event well enough.

There is also a class of events in data, consisting of uncorrelated sets of hits at the top and bottom of the detector. Neither of the two sets of hits is consistent with an upgoing hypothesis on its own, but coincidentally give an upward going track solution together. The estimation of how the measured light is distributed along the reconstructed track is useful for rejecting these events. The smoothness parameter is an indicator of how constant the light emission is along the track and these events can be removed by considering either the smoothness along the

track of the amplitude of the hits, or the smoothness of hits with time residual in the interval from −10 to 15 ns together with the likelihood of the Bayesian muon trajectory.

3.5. Filter level 6

The reconstructed zenith angle of the events, in the 421.9 days of data as well as in the equivalent of 421.9 days of simulated atmospheric neutrinos and atmospheric muons (renormalized from 483.2 days), that pass all the cuts is shown in Fig. 2. As there is no apparent excess of nearly vertically upgoing muons, we use the method of model rejection potential [23] in order to set the best limit on any potential WIMP signal. Assuming no signal, this is an unbiased way to select the final cut applied in an analysis by using Monte Carlo simulations of the experiment to calculate what the average upper limit would be if the measurement were repeated a large number of times. The natural variable for the optimization is the difference in the zenith angle of the reconstructed muon track between the neutralino signal events and the atmospheric neutrino background. The neutralino signal distribution has a sharp peak near the vertical while the distribution of the atmospheric neutrino events falls off towards the vertical.

The result is final zenith angle cuts for the various WIMP masses and annihilation channels ranging from 174.0° to 177.5°. The method of Feldman and Cousins [24] was used to calculate the 90% confidence level upper limits.

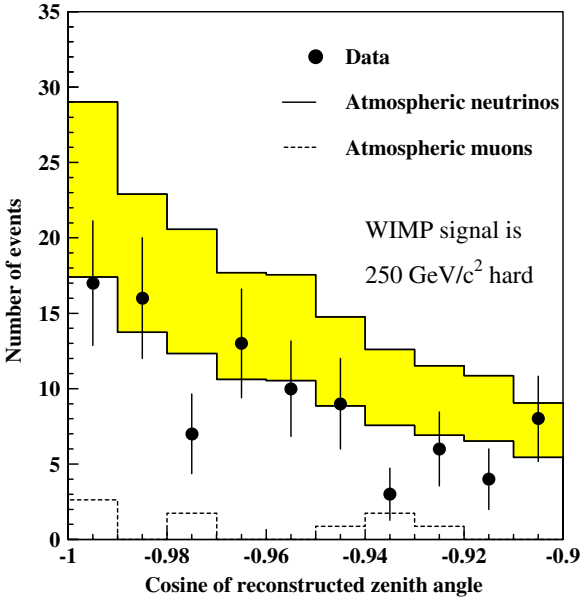

Fig. 2. The distribution of the cosine of the reconstructed zenith angle for 421.9 days of 1997–99 data (points) and atmospheric neutrino (shaded area) and muon simulations (dashed line) before the final cut in the $M_\chi = 250$ GeV/c^2 hard annihilation channel analysis. The shaded area of the atmospheric neutrino sample represents a ±25% systematic uncertainty.

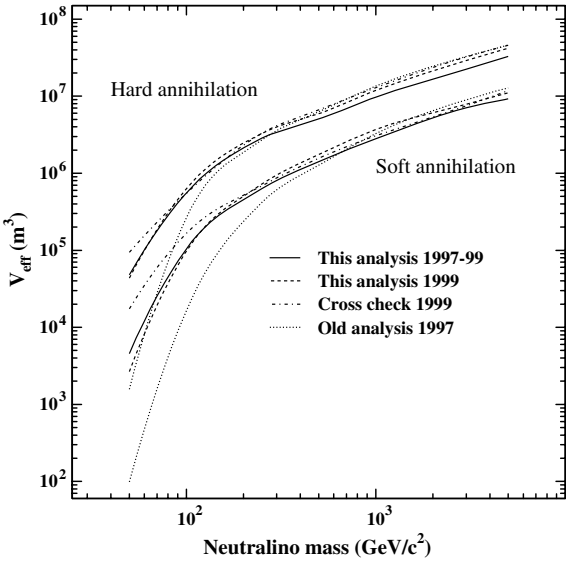

Fig. 3. The effective volume as a function of the neutralino mass for the simulated WIMP signal after the final filtering for both the hard (line) and the soft (dashed) annihilation channels. The result of the combined three year analysis is shown as well as a comparison between the 1999 part and the separate analysis performed on the 1999 data – presented in Section 4. Also shown is the effective volume for the previous analysis of the 1997 data [5].

The efficiency of each analysis can be represented by the effective volume for the signal

$$V_{\text{eff}} = V_{\text{gen}} \cdot N_{\text{L6}}/N_{\text{gen}}, \quad (1)$$

where N_{L6} is the number of WIMP signal events that pass the final cut and N_{gen} is the number of events originally generated in the volume V_{gen} around the detector. The

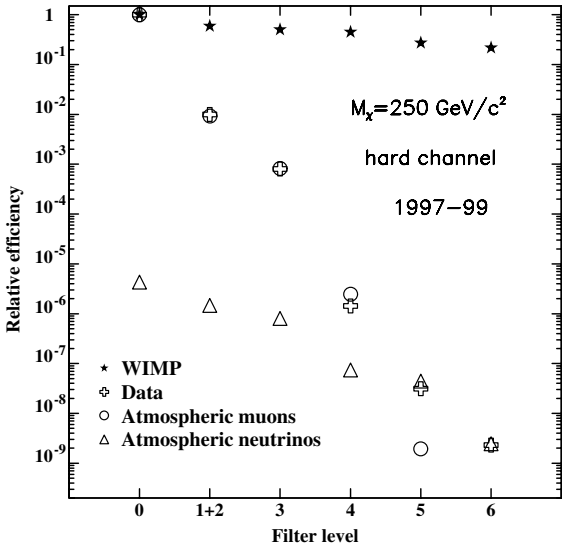

Fig. 4. The efficiencies relative to the trigger level for the combined data, WIMP signal, atmospheric muon and atmospheric neutrino simulations after the different filter levels in the $M_\chi = 250$ GeV/c^2 hard annihilation channel analysis. The atmospheric neutrinos have been normalized to the effective livetime of the experimental data.

effective volumes after the final zenith angle cut are shown in Fig. 3. The combined 1997–99 results are compared with those of the previous 1997 analysis [5]. For low masses there is a clear improvement in efficiency which mainly comes from the individual cut optimization for different masses and annihilation channels. The old 1997 analysis optimized the cuts for all masses using the 250 GeV/c^2 hard annihilation channel. Also shown in Fig. 3 is a comparison of the 1999 part of the current analysis with an independent analysis of the 1999 data presented in Section 4.

The passing rates for the various filter levels in the case of the 250 GeV/c^2 hard annihilation channel WIMP signal are presented in Table 1 as well as in Fig. 4.

4. Crosscheck

An independent analysis was performed using the data taken with the AMANDA detector during the austral winter of 1999. The effective livetime of the analyzed 1999 data set after rejection of runs with lower data quality was 221.4 days, corresponding to 1.3×10^9 triggers. This effective livetime was further reduced to 187.0 days or 1.1×10^9 triggers, because the subsample of 34.4 days that was used to tune the analysis cuts was not used in the final analysis to assure blindness.

In this analysis the downgoing atmospheric muon events and upgoing atmospheric neutrino events – of which 20×10^6 and 1.9×10^6 passed the trigger requirements, respectively – were simulated separately from the analysis described above. The simulated WIMP signal sample consisted of 14 subsamples of 5×10^5 events each. As before, two different annihilation channels were generated: $\chi\bar{\chi} \to W^+W^-$ as a reference hard neutrino spectrum and $\chi\bar{\chi} \to b\bar{b}$ as a reference soft neutrino spectrum with WIMPSIMP [8]. These two channels were simulated for seven different neutralino masses from 50 GeV/c^2 (in this case, the hard channel is $\chi\bar{\chi} \to \tau^+\tau^-$ and the soft channel is $\chi\bar{\chi} \to c\bar{c}$) to 5000 GeV/c^2, and the analysis was optimized independently for each of the 14 simulated signal samples.

The first part of the analysis focused on the rejection of the simulated downgoing muon events. A procedure was developed which selects the most sensitive variable to cut on (among a chosen set of 32 variables which parametrize the quality of an event, e.g. number of hit optical modules) and also determines the most optimal cut value. The following product is evaluated

$$\epsilon_{\text{signal}}(x; x_{\text{cut}})(1 - \epsilon_{\text{background}}(x; x_{\text{cut}})),$$

where ϵ_{signal} ($\epsilon_{\text{background}}$) is the fraction of signal (background) events which passes the cut x_{cut} in the variable x.

The calculation of $\epsilon_{\text{signal}}(1 - \epsilon_{\text{background}})$ as a function of x_{cut} results in a curve that peaks at cut values specific to the variables used. This cut value is taken as our optimal cut on the studied variable. The corresponding value of $\epsilon_{\text{signal}}(1 - \epsilon_{\text{background}})$ is used as a weight, estimating the efficiency of this variable with respect to others. The variable with the highest weight is taken for the first selection step and a cut is performed at the optimal cut value. After this, the same procedure is executed for all the remaining variables. Consecutive cuts are chosen using this method until all the simulated downgoing atmospheric muon events have been rejected, see Ref. [6] for more details on the selection procedure.

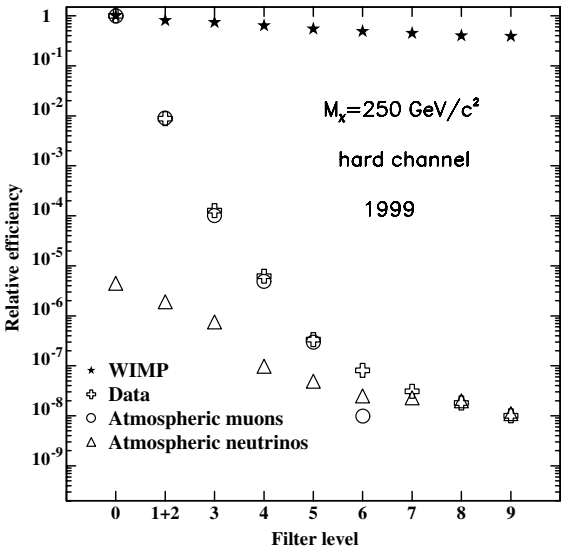

Fig. 5. The relative efficiency of the selection procedure as function of the analysis cuts for the experimental data, simulated signal events ($M_\chi = 250$ GeV/c^2 hard annihilation channel) and simulated background events (atmospheric muons and atmospheric neutrinos). All samples have been normalized to 1 at trigger level, except that the atmospheric neutrinos have been normalized to the effective livetime of the experimental data. 'Filter level n' ($n > 2$) corresponds to the $(n-2)$th cut of the selection procedure described.

After several cuts the data consists only of upgoing atmospheric neutrinos and a possible WIMP signal. This is illustrated in Fig. 5. As we see no evidence for a WIMP signal, an upper limit on the muon flux coming from the annihilation of the neutralinos at the center of the Earth can be calculated. The method of model rejection potential was applied, as in Section 3.5. Several variables were tried for the last cut, and the zenith angle was selected as it gave the best rejection factor. The effective volume for the simulated signal samples after all cuts is shown in Fig. 3. The two separate analyses of the 1999 data achieve about the same efficiency, except for the 50 GeV/c^2 neutralino mass where the individual optimisation in this analysis proves fruitful.

5. Results

5.1. Systematic uncertainties

The inclusion of systematic uncertainties in the signal and background estimate in the limit calculations is done using the POLE program [25,26] which is a generalisation of the method proposed in Ref. [27]. The calculation takes into account the uncertainty in the signal detection effi-

ciency as well as both the theoretical uncertainty and the uncertainty in detection efficiency for the background.

The theoretical uncertainty in the atmospheric neutrino flux calculation is estimated to be ~20% [28,29] and a conservative assumption of ±25% is used.

The systematic uncertainty in the detection efficiency is dominated by three contributions: OM sensitivity, muon energy loss and the implementation of the ice properties in the detector simulation.

The uncertainty in the OM sensitivity has been estimated to be around 20%. It is due to a combination of effects like the properties of the refrozen ice close to the OM, the quantum efficiency and the transmissivity of the glass and the optical gel. Monte Carlo simulation studies of atmospheric neutrinos have shown that this translates into an uncertainty in the muon rate of about 30% for muons in the energy range 10^2–10^3 GeV.

The simulation of the muon propagation to the detector has an uncertainty in the muon range which is less than 10%. The muon flux at the detector is proportional to the range of the muon [9] and therefore a systematic uncertainty of 10% on the number of muons is used.

The uncertainty in the detection efficiency due to the implementation of the ice properties in the detector simulation has been estimated by using two different ice models in the simulation of the neutralino signal as well as in the atmospheric neutrino background. The signal has a fairly uniform uncertainty of 8–10% independent of the neutralino mass and annihilation channel, although the 100 GeV/c^2 hard and soft annihilation channels have the highest values of 12% and 20%, respectively. In contrast the atmospheric neutrino background have the lowest uncertainty for the 100 GeV/c^2 channels – 8% (hard) and 11% (soft) – while it ranges between 15% and 25% in the other cases.

Neutrino oscillations of the type $\nu_\mu \to \nu_\tau$ would reduce the sensitivity to WIMP annihilations. Because of the relatively high neutrino energy threshold of AMANDA (~35 GeV), this effect is completely negligible, however, for all considered WIMP masses.

Added in quadrature this yields systematic uncertainties between 33% and 40% depending on the WIMP analysis considered.

5.2. Flux limits and comparisons

The 90% confidence level upper limit μ_{90} on the number of muons with energies above $E_{\rm thr}$ coming from annihilating neutralinos together with the effective volume $V_{\rm eff}$ and the experimental livetime $T_{\rm eff}$ limits the conversion rate of neutrinos into muons per unit volume and time around the detector

$$\Gamma_{\mu\nu} \leqslant \frac{\mu_{90}}{V_{\rm eff} \cdot T_{\rm eff}}. \tag{2}$$

This rate is directly proportional to the annihilation rate $\Gamma_{\rm A}$ [5] through

$$\Gamma_{\mu\nu} = \Gamma_{\rm A} \cdot \frac{1}{4\pi R_\oplus^2} \int {\rm d}E_\nu \sigma_{\nu N}(E_\nu) \rho_{\rm N} {\rm BR}_{\chi\bar{\chi}\to X} \left(\frac{{\rm d}N}{{\rm d}E_\nu}\right)_X, \tag{3}$$

where $R_\oplus$ is the radius of the Earth, $\sigma_{\nu N}$ is the neutrino–nucleon cross section, $\rho_{\rm N}$ is the nucleon density in the ice around the detector and ${\rm BR}_{\chi\bar{\chi}\to X}$ is the branching ratio for the neutralino annihilation with associated neutrino spectrum $({\rm d}N/{\rm d}E_\nu)_X$.

Since the detector thresholds and efficiencies are taken into account in the calculation of the annihilation rate limits these are directly comparable to those of other experiments.

The neutralino annihilation rate at the center of the Earth is then used to calculate the 90% confidence level upper limit on the muon flux ϕ_μ for any given energy threshold $E_{\rm thr}$ [5]

$$\phi_\mu(E_\mu \geqslant E_{\rm thr}) = \frac{\Gamma_{\rm A}}{4\pi R_\oplus^2} \int_{E_{\rm thr}}^{\infty} {\rm d}E_\mu \frac{{\rm d}N}{{\rm d}E_\mu}, \tag{4}$$

where the differential term ${\rm d}N/{\rm d}E_\mu$ includes all the assumptions necessary to account for the production of muons from neutrinos created by neutralino annihilations as well as the propagation of those muons to the detector. In order to compare the results in this paper with published results of other experiments, a threshold of 1 GeV is used. The conversion factors used with Eqs. (3) and (4) for converting $\mu_{90} \to \Gamma_{\rm A} \to \phi_\mu$ have been calculated with code based on simulations presented in [8].

The 90% confidence level upper limits on the muon flux from neutralino annihilations at the center of the Earth for the 421.9 day data set obtained during the three year period 1997–99 as well as the upper limits on the annihilation rate of neutralinos are presented in Table 3. In Fig. 6 the upper limits on the muon flux for the seven different neutralino masses and the two annihilation channels are plotted. The corresponding limits calculated without the inclusion

Table 3
The 90% confidence level upper limits on the annihilation rate $\Gamma_{\rm A}$ and the muon flux ϕ_μ calculated with the inclusion of systematic uncertainties for the combined 1997–99 data analyses

Channel	M_χ (GeV/c^2)	$N_{\rm data}$	$N_{{\rm atm.}\nu}$	μ_{90}	$\Gamma_{\rm A}$ (s^{-1})	ϕ_μ (km^{-2} year^{-1})
Hard	50	11	13.7	8.5	3.7×10^{15}	1.4×10^{4}
	100	11	13.7	8.5	8.1×10^{13}	1.8×10^{3}
	250	9	9.6	8.9	5.9×10^{12}	9.4×10^{2}
	500	4	5.0	5.3	9.1×10^{11}	5.6×10^{2}
	1000	2	4.0	2.9	1.3×10^{11}	3.0×10^{2}
	3000	2	3.0	3.5	2.3×10^{10}	3.4×10^{2}
	5000	2	3.1	3.5	9.4×10^{09}	3.2×10^{2}
Soft	50	10	13.1	8.1	2.7×10^{17}	2.0×10^{5}
	100	10	13.1	8.1	2.1×10^{15}	6.6×10^{3}
	250	12	10.6	12.7	1.4×10^{14}	2.5×10^{3}
	500	6	7.2	6.5	1.4×10^{13}	8.8×10^{2}
	1000	4	5.1	5.3	3.2×10^{12}	6.3×10^{2}
	3000	3	4.7	3.9	3.8×10^{11}	3.9×10^{2}
	5000	2	4.1	2.9	1.5×10^{11}	3.0×10^{2}

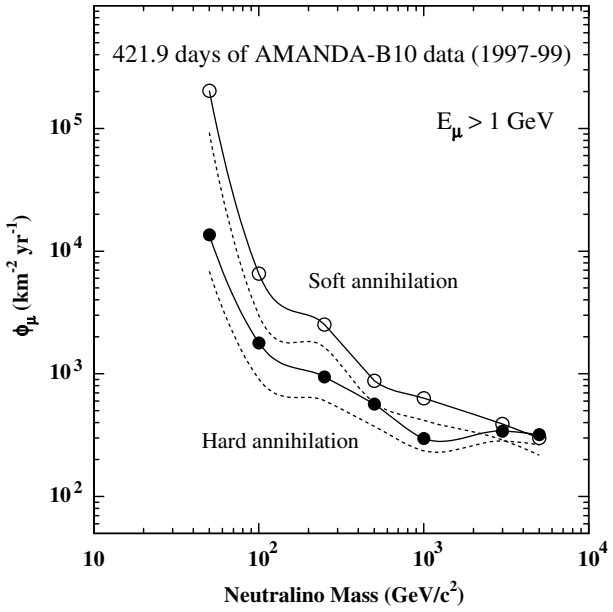

Fig. 6. The upper limits on the muon flux from neutralino annihilations at the center of the Earth for the combined 1997–99 data corresponding to 421.9 days of livetime. The lines are to guide the eye. The limits obtained without the inclusion of systematic uncertainties are shown for comparison as dotted lines.

of systematic uncertainties are shown as dotted lines for comparison.

A comparison of the AMANDA upper limits on the muon flux from neutralino annihilations at the center of the Earth with earlier results [5] as well as four other collaborations (Baksan [30], Macro [31], Super-Kamiokande [32], and Baikal [33]) is shown in Fig. 7. In that figure the predictions of theoretical models are also presented, which include new estimates on the WIMP diffusion in the solar system [35]. The MSSM models disfavored by the recent measurement of the CDMS collaboration [34] in the Soudan Underground Laboratory are indicated by dots.

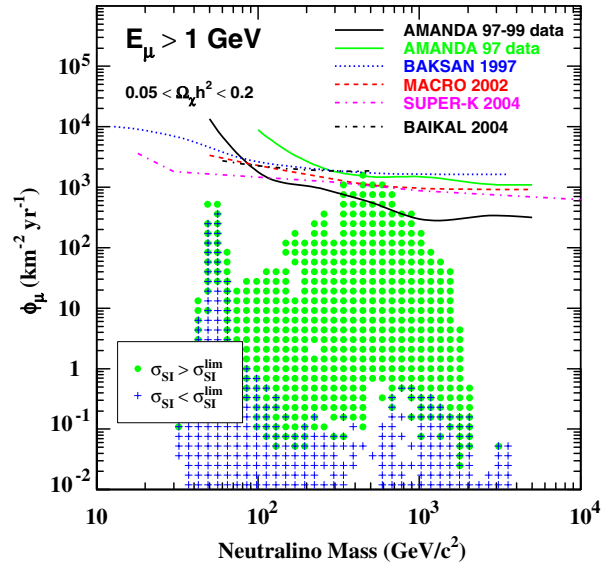

Fig. 7. The AMANDA limits on the muon flux from the hard neutralino annihilation channels at the center of the Earth for the three year 1997–99 combined data set compared with earlier results [5] and those of Baksan [30], Macro [31], Super-Kamiokande [32], and Baikal [33]. MSSM model predictions with new estimates on the WIMP diffusion in the solar system [35] are also shown, with the dots indicating models that are disfavored by CDMS [34]. The plus signs mark those not probed by CDMS.

6. Conclusions

A search has been performed for nearly vertically upward going muons with AMANDA data from the three years 1997–99. Such muons could be a signature of dark matter in the form of neutralinos accumulating and annihilating at the center of the Earth. The number of muons found, as well as their angular distribution, is compatible with the expected background induced by atmospheric neutrinos. The results have been used to derive limits as a function of neutralino mass on the neutralino annihilation rate and the neutrino-induced muon flux.

The limits obtained in this analysis are the best so far for indirect neutralino searches at high masses, even though the livetime of 421.9 days is lower than that of the published results of other collaborations. Direct detection experiments which set limits on the spin-independent neutralino–nucleon cross section are sensitive to high velocity particles. Indirect experiments, like AMANDA, require low velocity neutralinos being trapped by the gravitational field of the Earth or the Sun. In this sense the two methods are complementary, since they would sample different populations of dark matter. Although taking into account WIMP diffusion in the solar system has lowered the expected theoretical muon flux significantly [35], the indirect searches have now begun to probe regions allowed by theoretical models with supersymmetric dark matter candidates as is shown in Fig. 7.

The data analyzed here are of particular interest in the search for low energy neutrino-induced muons because of the low multiplicity trigger thresholds used during the 1997–1999 seasons.

Acknowledgements

We acknowledge the support from the following agencies: National Science Foundation-Office of Polar Program, National Science Foundation-Physics Division, University of Wisconsin Alumni Research Foundation, Department of Energy, and National Energy Research Scientific Computing Center (supported by the Office of Energy Research of the Department of Energy), the NSF-supported TeraGrid system at the San Diego Supercomputer Center (SDSC), and the National Center for Supercomputing Applications (NCSA); Swedish Research Council, Swedish Polar Research Secretariat, High Performance Computing Center North (HPC2N), National Supercomputer Centre, and Knut and Alice Wallenberg Foundation, Sweden; German Ministry for Education

and Research, Deutsche Forschungsgemeinschaft (DFG), Germany; Fund for Scientific Research (FNRS-FWO), Flanders Institute to encourage scientific and technological research in industry (IWT), Belgian Federal Office for Scientific, Technical and Cultural affairs (OSTC); the Netherlands Organisation for Scientific Research (NWO); M. Ribordy acknowledges the support of the SNF (Switzerland); J.D. Zornoza acknowledges the Marie Curie OIF Program (contract 007921).

References

[1] D.N. Spergel et al., Astrophys. J. Suppl. Ser. 148 (2003) 175.
[2] L. Bergström, J. Edsjö, P. Gondolo, Phys. Rev. D 55 (1997) 1765.
[3] E. Andrés et al., Astrop. Phys. 13 (2000) 1.
[4] P. Ekström, Ph.D. thesis, Stockholm University, 2004.
[5] J. Ahrens et al., Phys. Rev. D 66 (2002) 032006.
[6] P. Olbrechts, Ph.D. thesis, Vrije Universiteit Brussel, 2004.
[7] Y. Minaeva, Ph.D. thesis, Stockholm University (2004); Amanda Collaboration, Astrop. Phys. 24 (2006) 459.
[8] L. Bergström, J. Edsjö, P. Gondolo, Phys. Rev. D 58 (1998) 103519.
[9] J. Edsjö, Ph.D. thesis, Uppsala University, 1997.
[10] T. Sjöstrand et al., Comput. Phys. Commun. 135 (2001) 238.
[11] G.C. Hill, Astropart. Phys. 6 (1997) 215.
[12] A.D. Martin, W.J. Stirling, R.G. Roberts, Phys. Lett. B 354 (1995) 155.
[13] D. Heck et al., FZKA Report No. 6019, Forschungszentrum Karlsruhe, 1998.
[14] J. Wentz et al., Phys. Rev. D 67 (2003) 073020.
[15] B. Wiebel-Sooth, Ph.D. thesis, Universität Wuppertal, 1998.
[16] N.N. Kalmykov, S.S. Ostapchenko, Phys. At. Nucl. 56 (1993) 346; N.N. Kalmykov, S.S. Ostapchenko, A.I. Pavlov, Bull. Russ. Acad. Sci. 58 (1994) 1966 (Physics).
[17] D.A. Chirkin, Ph.D. thesis, University of California at Berkeley, 2003. D. Chirkin, W. Rhode, in: Proceedings of the XXVII International Cosmic Ray Conference (ICRC), 2001, p. 1017.
[18] A. Karle, in: C. Spiering (Ed.). Simulation and Analysis Methods for Large Neutrino Telescopes, (DESY-PROC-1999-01, 1999), p. 174.
[19] K. Woschnagg et al., in: Proceedings of the XXVI International Cosmic Ray Conference (ICRC), 1999, p. HE.4.1.5.
[20] S. Hundertmark, in: C. Spiering (Ed.). Simulation and Analysis Methods for Large Neutrino Telescopes, (DESY-PROC-1999-01, 1999), p. 276.
[21] J. Ahrens et al., Nucl. Instrum. Meth. A 524 (2004) 169.
[22] J. Schwindling and B. Mansoulié (2000). Available from:<http://schwind.home.cern.ch/schwind/MLPfit.html>.
[23] G.C. Hill, K. Rawlins, Astropart. Phys. 19 (2003) 393.
[24] G.J. Feldman, R.D. Cousins, Phys. Rev. D 57 (1998) 3873.
[25] J. Conrad, O. Botner, A. Hallgren, C. Pérez de los Heros, Phys. Rev. D 67 (2003) 012002.
[26] J. Conrad, Comp. Phys. Comm. 158 (2004) 117.
[27] R.D. Cousins, V.L. Highland, Nucl. Instrum. Meth. A 320 (1992) 331.
[28] T.K. Gaisser, Proceedings of the Nobel Symposium 129 on Neutrino Physics Enköping, Sweden, 19–24 August 2004, in: L. Bergström et al. (Eds.), Physica Scripta T121 (2005) 51.
[29] T.K. Gaisser, M. Honda, Ann. Rev. Nucl. Part. Sci. 52 (2002) 153.
[30] M. Boliev et al., in: H.V. Klapdor-Kleingrothaus, Y. Ramachers (Eds.), Proceedings of Dark Matter in Astro- and Particle Physics, World Scientific, 1997, p. 711; O. Suvorova. Available from: <hep-ph/9911415>.
[31] M. Ambrosio et al., Phys. Rev. D 60 (1999) 082002.
[32] S. Desai et al., Phys. Rev. D 70 (2004) 083523; S. Desai et al., Phys. Rev. D 70 (2004) 109901.
[33] V. Aynutdinov et al., Nucl. Phys. B 143 (2005) 335 (Proc.Suppl.).
[34] D.S. Akerib et al., Phys. Rev. Lett. 93 (2004) 211301; D.S. Akerib et al., Phys. Rev. Lett. 96 (2006) 011302.
[35] J. Lundberg, J. Edsjö, Phys. Rev. D 69 (2004) 123505.